



Volume 24

February 2007

ISSN 0013-780X

SIGNAL PROCESSING

IMAGE COMMUNICATION

Theory, Techniques & Applications

A SUBSCRIPTION SERVICE AVAILABLE TO QUALIFYING MEMBERS

Member Price: \$100/Year
Student Price: \$50/Year



Aims and scope

Signal Processing: Image Communication is an international journal for the development of the theory and practice of **image communication**. Its primary objectives are the following:

To present a forum for the advancement of theory and practice of image communication.

To stimulate cross-fertilization between areas similar in nature which have traditionally been separated, for example, various aspects of **visual communications** and **information systems**.

To contribute to a rapid information exchange between the industrial and academic environments.

The editorial policy and the technical content of the journal are the responsibility of the Editor-in-Chief, the Area **Editors** and the Advisory Editors. The Journal is self-supporting from subscription income and contains a minimum amount of advertisements. Advertisements are subject to the prior approval of the Editor-in-Chief. The journal welcomes contributions from every country in the world.

Signal Processing: Image Communication publishes articles relating to aspects of the design, implementation and use of **image communication systems**. The journal features original research work, tutorial and review articles, and accounts of practical developments.

Subjects of interest include image/video coding, 3D video representations and compression, 3D graphics and animation compression, HDTV and 3DTV systems, video adaptation, video over IP, peer-to-peer video networking, interactive visual communication, multi-user video conferencing, wireless video broadcasting and communication, visual surveillance, 2D and 3D image/video quality measures, pre/post processing, video restoration and super-resolution, multi-camera video analysis, motion analysis, content-based image/video indexing and retrieval, face and gesture processing, video synthesis, 2D and 3D image/video acquisition and display technologies, architectures for image/video processing and communication.

Editor-In-Chief

A. Cavallaro

Queen Mary University of London School of Electronic Engineering and Computer Science, Mile End Road, E1 4NS, London, United Kingdom

Area Editors

G. Alregib

Georgia Institute of Technology School of Electrical and Computer Engineering, Atlanta, Georgia, United States of America

O. Alshaykh

Boston University, Boston, Massachusetts, United States of America

P. K. Atrey

University at Albany, Albany, New York, United States of America

I. Bajic

Simon Fraser University, Burnaby, British Columbia, Canada

F. Battisti

Roma Tre University, Roma, Italy

A. Beghdadi

Sorbonne North Paris University, Villetaneuse, France

J. Benois-Pineau

Bordeaux Computer Research Laboratory, Talence, France

G. Boato

University of Trento, Department of Information Engineering and Computer Science, Povo, Italy

K. Brunnström

RISE Research Institutes of Sweden AB, Göteborg, Sweden

M. Cagnazzo

Télécom Paris, Paris, France

R. Caldelli

University of Florence, Firenze, Italy

M. Carli

Roma Tre University, Roma, Italy

X. Chen, PhD

University of Science and Technology of China, Hefei, Anhui, China

W.-H. Cheng

National Yang Ming Chiao Tung University, Hsinchu, Taiwan

G. Cheung

York University, Toronto, Ontario, Canada

S. Cheung

University of Kentucky, Lexington, Kentucky, United States of America

S. Coulombe

École de technologie supérieure, Montréal, Quebec, Canada

T. Dagiuklas

London South Bank University, London, United Kingdom

J. Dittmann

Otto von Guericke University, Magdeburg, Germany

Y. Fang

Jiangxi University of Finance and Economics, Nanchang, China

S. Faria

Institute for Telecommunications Delegation of Leiria, Leiria, Portugal

M. Farias

University of Brasilia, Department of Electrical Engineering, BRASILIA, Brazil

R. Farrugia

University of Malta, Msida, Malta

K. Gu

Beijing University of Technology, Beijing, China

F. Hartung, Dr.-Ing.

FH Aachen University of Applied Sciences, Aachen, Germany

A.T.S. Ho

University of Surrey, Guildford, United Kingdom

J. Hou, PhD

City University of Hong Kong, Department of Computer Science, Hong Kong, Hong Kong

A. Iosifidis

Aarhus University, Department of Electrical and Computer Engineering, Aarhus, Denmark

X. Kang

Sun Yat-Sen University, Guangzhou, China

Y. Kompatsiaris

Centre for Research and Technology-Hellas, Thessaloniki, Greece

J. Konrad

Boston University, Boston, Massachusetts, United States of America

A. Koz

Middle East Technical University, Ankara, Turkey

M. Larabi

University of Poitiers, Poitiers, France

J.S. Lee

Yonsei University, Seodaemun-gu, South Korea

H. Li

University of Electronic Science and Technology of China, Chengdu, Sichuan, China

W. Lin

Shanghai Jiao Tong University - Fahu Campus, Shanghai, China

H. Liu

Cardiff University, Cardiff, United Kingdom

Z. Liu

Shanghai University, Shanghai, China

B. Macchiavello

University of Brasilia, BRASILIA, Brazil

J. Meng, PhD

University at Buffalo, Department of Computer Science and Engineering, Buffalo, New York, United States of America

M. Mitrea

TELECOM SudParis, Evry, France

N. Nikolaidis

Aristotle University of Thessaloniki, Thessaloniki, Greece

F. Odone

University of Genoa, MaLGa Machine Learning Genoa Center, Genova, Italy

N. O'Connor

Dublin City University, Dublin, Ireland

F. Pereira

University of Lisbon Higher Technical Institute, Lisboa, Portugal

W. Puech

University of Montpellier, Montpellier, France

C. Qin

University of Shanghai for Science and Technology, Shanghai, China

N. Ramzan

University of the West of Scotland, , United Kingdom

H. Sahbi

Sorbonne University, Paris, France

P. Schelkens

VUB University, Brussel, Belgium

V. Stankovic

University of Strathclyde, Glasgow, United Kingdom

X. Sun

Microsoft Research Asia, Beijing, China

A. Tefas

Aristotle University of Thessaloniki, Thessaloniki, Greece

C. Timmerer

Alpen-Adria University, Klagenfurt, Austria

A. Uhl

Paris Lodron University of Salzburg, Salzburg, Austria

G. Valenzise

National Centre for Scientific Research, Paris, France

V. Velisavljevic

University of Bedfordshire, Luton, United Kingdom

M. Wang

Hefei University of Technology, Hefei, China

M. Wien

RWTH Aachen University, Aachen, Germany

G. S. Xia, PhD

Wuhan University, Wuhan, China

Y. Zhao

Beijing Jiaotong University, Beijing, China

Y. Zhou

University of Macau, Taipa, Macao

C. Zhu

University of Electronic Science and Technology of China School of Electronic Science and Engineering, Chengdu, Sichuan, China

All members of the Editorial Board have identified their affiliated institutions or organizations, along with the corresponding country or geographic region. Elsevier remains neutral with regard to any jurisdictional claims.

Research article ● Full text access

CAM-based HDR image reproduction using CA–TC decoupled JCh decomposition

Hyuk-Ju Kwon, Sung-Hak Lee

Pages 1-13

[Download PDF](#) [Article preview](#) ▼

Research article ● Full text access

Temporal stochastic linear encoding networks

Zhigang Zhu, Hongbing Ji, Wenbo Zhang, Guopeng Huang

Pages 14-20

[Download PDF](#) [Article preview](#) ▼

Research article ● Full text access

An alternating proximal approach for blind video deconvolution

Feriel Abboud, Émilie Chouzenoux, Jean-Christophe Pesquet, Jean-Hugues Chenot, Louis Laborelli

Pages 21-36

[Download PDF](#) [Article preview](#) ▼

Research article ● Full text access

Perceptual image quality assessment through spectral analysis of error representations

Dogancan Temel, Ghassan AlRegib

Pages 37-46

[Download PDF](#) [Article preview](#) ▼

Research article ● Full text access

Fast detection and segmentation of partial image blur based on discrete Walsh–Hadamard transform

Xuewei Wang, Xiao Liang, Jinjin Zheng, Hongjun Zhou

Pages 47-56

[Download PDF](#) [Article preview](#) ▼

Research article ● Full text access

A framework for computationally efficient video quality assessment

Wellington Y.L. Akamine, Pedro Garcia Freitas, Mylène C.Q. Farias

Pages 57-67

[Download PDF](#) [Article preview](#) ▼

Research article ● Full text access

Multiview Laplacian semisupervised feature selection by leveraging shared knowledge among multiple tasks

Ganesh Krishnasamy, Raveendran Paramesran

Pages 68-78

[Download PDF](#) [Article preview](#) 

Research article ● Full text access

HybridNet: A fast vehicle detection system for autonomous driving

Xuerui Dai

Pages 79-88

[Download PDF](#) [Article preview](#) 

Research article ● Full text access

Combining weighted curvelet accumulation with motion vector duty cycle for nonuniform video deblurring

Jing Li, Weiguo Gong, Huimei Zhan, Weihong Li

Pages 89-103

[Download PDF](#) [Article preview](#) 

Research article ● Full text access

Digital blind watermarking based on depth variation prediction map and DWT for DIBR free-viewpoint image

Yong-Seok Lee, Young-Ho Seo, Dong-Wook Kim

Pages 104-113

[Download PDF](#) [Article preview](#) 

Mini review ● Open access

Signal processing challenges for digital holographic video display systems

David Blinder, Ayyoub Ahar, Stijn Bettens, Tobias Birnbaum, ... Peter Schelkens

Pages 114-130

[Download PDF](#) [Article preview](#) 

Research article ● Full text access

Image dehazing using Moore neighborhood-based gradient profile prior

Dilbag Singh, Vijay Kumar

Pages 131-144

[Download PDF](#) [Article preview](#) 

Research article ● Full text access

Object instance detection with pruned Alexnet and extended training data

Rui Wang, Jingwen Xu, Tony X. Han

Pages 145-156

[Download PDF](#) [Article preview](#) 

Research article ● Full text access

ADMM for image restoration based on nonlocal simultaneous sparse Bayesian coding

Xiaolei Lu, Xuebin Lü

Pages 157-173

[Download PDF](#) [Article preview](#) 

Research article ● Full text access

Lossless medical image watermarking method based on significant difference of cellular automata transform coefficient

Tzuo-Yau Fan, Her-Chang Chao, Bin-Chang Chieu

Pages 174-183

[Download PDF](#) [Article preview](#) 

Research article ● Full text access

Deep learning for printed document source identification

Min-Jen Tsai, Yu-Han Tao, Imam Yuadi

Pages 184-198

[Download PDF](#) [Article preview](#) 

Research article ● Full text access

Fast inter-frame prediction in multi-view video coding based on perceptual distortion threshold model

Gangyi Jiang, Baozhen Du, Shuqing Fang, Mei Yu, ... Fen Chen

Pages 199-209

[Download PDF](#) [Article preview](#) 

Research article ● Full text access

A deep learning method for image super-resolution based on geometric similarity

Jian Lu, Weidong Hu, Yi Sun

Pages 210-219

[Download PDF](#) [Article preview](#) 

Research article Full text access

A fast video super resolution for facial image

Mahmood Amiri, Alireza Ahmadyfard, Vahid Abolghasemi

Pages 259-270

[Download PDF](#) [Article preview](#) 

Research article Full text access

Saliency detection via background and foreground null space learning

Ying Ying Zhang, Shuo Zhang, Ping Zhang, XinGang Zhang

Pages 271-281

[Download PDF](#) [Article preview](#) 



Deep learning for printed document source identification

Min-Jen Tsai^{a,*}, Yu-Han Tao^a, Imam Yuadi^{a,b}

^a National Chiao Tung University, Institute of Information Management, 1001 Ta-Hsueh Road, Hsin-Chu, 300, Taiwan, ROC

^b Airlangga University, Department of Information and Library Science, Jl. Airlangga 4-6 Surabaya 60286, East Java, Indonesia

ARTICLE INFO

Keywords:

Printer source identification
Machine learning
Deep learning
Convolutional neural networks

ABSTRACT

Due to the rapid development of the information technology and wide use of the Internet, Information is easily to be obtained in the form of digital format. Digital content can be freely printed into documents since the convenience and accessibility of the printers. On the other hand, printed documents can be illegally manipulated by some criminal issues such as: forged documents, counterfeit currency, copyright infringement, and so on. Therefore, how to develop an efficient and appropriate safety testing tool to identify the source of printed documents is an important task in the meantime. Currently, the forensic system using the statistical methods and support vector machine technology has been able to identify the source printer for the text and the image documents. Such an approach belongs to the category of shallow machine learning with human interaction during the stages of feature extraction, feature selection and data pre-processing. In this paper, a deep learning system to solve the complex image classification problem is developed by Convolutional Neural Networks (CNNs) of deep learning which can learn the features automatically. Systematic experiments have been performed for both systems. For microscopic documents, feature based SVM system outperforms the deep learning system with limited gap. For scanned documents, both system can achieve equally well with high accuracy. Both systems should be constantly evaluated and compared for the best interest in universal utilization.

1. Introduction

Owing to the advances of new information technology and Internet development, digital contents are widely used over the world. The techniques of digital image processing are also applied to many areas such as Medical Science, Biology, Engineer Science, Cryptography, E-commerce... etc. Even digital format is highly circulated, printed documents are still popularly accepted and easily distributed since the printer has become the commodity product. However, these devices give the potential effects where the printed digital documents often contain information about crimes committed like forgery, fabricating documents, fabricating lottery or bills ... etc. Since the criminal counterfeits and copyright infringement is still under study for the new media, there is a need to identify the printer source.

In principle, digital forensics is the technology which is associated with legal issues to identify, collect, analyze and examine digital evidence to prove the appearance of a crime [1]. Therefore, appropriate techniques and materials are needed to identify forensic object accurately and precisely during the forensic investigation [2,3]. In general, an appropriate method will be able to determine the source of the document since each printer has distinctive textural characteristics than others. For example, drifting motor and precision gear during the printing process have created the pattern information from a printer which can be used as the intrinsic signatures of these devices. Accordingly,

every printer has characteristic signatures based on a corresponding fluctuation in developed toner on the printed pages.

Previous studies commonly extracted the statistical features [4,5] from the printed documents by Local Binary Pattern (LBP), Gray-Level Co-Occurrence Matrix (GLCM), Discrete Wavelet Transform (DWT), spatial filters ... etc. for feature extraction. Subsequently, support vector machine (SVM) [6] is adopted for the forensic classification system. However, above mentioned approaches require significant human involvement with expert knowledge during the procedures of feature extraction, feature selection and classification. In addition, it is necessary to repeat the whole processes several times with random selection of training and testing samples in order to get the generalized results. Therefore, quite an amount of time expense is needed. This research will utilize not only high resolution scanners but also the high magnification optical microscope to get the clear texture information from either texts or images.

On the other hand, machine learning techniques have been dramatically changed the whole research field for academic institution and industry. Machine learning is a subfield of artificial intelligence (AI) [7]. The goal of machine learning generally is to understand the structure of data and fit that data into models that can be understood and utilized. Deep Learning is a new area of Machine Learning research and uses many-layered Deep Neural Networks (DNNs) to learn levels of

* Corresponding author.

E-mail address: mjtsai@cc.nctu.edu.tw (M.-J. Tsai).

representation and abstraction that make sense of data such as images, sound, and text. Moreover, convolutional neural networks (CNNs) [8] recently have shown to be very effective in complex image classification tasks in machine learning field. The main benefit of using CNNs with respect to traditional fully-connected neural networks is the reduced amount of parameters to be learned. Convolutional layers made of small size kernels are an effective way to produce high-level features that are fed to fully-connected layers and significantly reduce the computation time with high accuracy rate.

Under such consideration, this paper intends to leverage the technology advancement of deep learning for source printer identification, which can reduce the burden of human machine interaction with automatic classification capability. To achieve those goals, the objective of this paper is to obtain the best performance for printer source identification for text and natural image documents where the deep learning technique is utilized. Furthermore, the aim of the research is also to compare the best decision results from machine learning with the existing techniques.

As a consequence, this paper is organized as following: Section 2 describes the related works, classification techniques, deep learning methodology and feature based approach. Section 3 presents the proposed technique used in this study. In Section 4, experimental results are reported with discussion, and Section 5 concludes the paper with areas of possible future investigation.

2. Related works, deep learning methodology and feature filter based SVM classification

2.1. Related works

Printed documents generated from different laser printers will produce differences of texture structure either for printed text or images on the paper, in general with a toner cartridge. Toner particles are specifically melted by the heat of the fuser, and are thus bonded to the paper. The intrinsic signatures from the printer, which can be detected on a document paper including shapes, sizes and patterns can be used as a guide for researchers to distinguish and classify the printer sources [9–18]. There are several approaches for authenticating printed documents and Table 1 illustrates the literature papers on the associated topics for source identification. Mikkilineni et al. [19,20] applied GLCM for each English “e” character to form the feature vectors. In their experiment [19], two strategies were developed for printer identification based on examining the printed document. Finding intrinsic signatures of the printed document was the first solution for identifying the characteristics of a particular printer, model and manufacturer’s brand with very high resolution (2400 dpi). Meanwhile, the other one was banding by detecting the extrinsic signature with embedded information from a document with electrophotography (EP) printers in modulating the intrinsic feature. They implemented a 5-Nearest-Neighbor (5NN) classifier in their previous work [19,20] and in other experiments [9,18], SVM was applied to classify 10 printer types. Several researchers in [10–12] also conducted their experiments by using GLCM with different approaches with extended features. Tsai et al. [10,11] implemented GLCM and DWT based feature extraction to identify Chinese character and used feature selection to get the optimum feature set for printer source identification. In further study, Kee and Farid [14] proposed two solutions using principal component analysis (PCA) and singular value decomposition (SVD) for printed characters to distinguish source printers. Wu et al. [15] extracted the geometric distortion of Chinese document as the intrinsic features for classification.

On the other hand, examinations of intrinsic marks for image document were conducted with various techniques. Choi et al. [16] used the noise features extracted from the statistical analysis of the HH sub-band of DWT for 15 RGB channel features and 24 Cyan, Magenta, Yellow and Black (CMYK) channel features for identifying the source of color laser printer. Alternatively, Kim and Lee [17] applied each CMY color

Table 1
Research papers on the topic of identifying printed document.

Document type	Research	Approach	Research object	Classifier	Claimed average accuracy rate	Number of printers
Text document	[9]	GLCM	English character “e”	SVM	93.0%	10
	[10]	GLCM, DWT	Chinese character “永”	SVM	98.64%	12
	[12]	GLCM, MDMS, GLCM_MD, CTGF_GLCM, MDMS and others	English character “e” and frame document	SVM	97.60%	10
	[13]	CNN	English character “a”, “e” and frame document	Machine learning	97.33%	10
Natural image document	[16]	DWT, GLCM	Color image document	SVM	88.75%	8
	[17]	Discrete Fourier transform (DFT)	Photograph Image document	SVM	94.4%	7
	[18]	Hough transform	Photograph Image document	*	91.9%	9

Note: * denotes no exact information provided.

channel in the discrete Fourier transform (DFT) domain to identify the color laser printer. Accordingly, Ryu et al. [18] investigated the property of halftone textures from electrophotographic printer in each channel of CMYK domain. They applied the Hough transform and constructed the histogram by angle values. Correspondingly, Bulan et al. [21] also assessed the similarity of a pair of geometric distortion signatures during the printing process using the normalized correlation.

Use of multi-dimensional and multi-scale GLCM features for printer classification was proposed in [12]. This method applied the scheme on selected individual letter “e”, a portion of a document (termed as ‘frames’) as the training data. SVM classifier was applied and the highest average accuracy reported in [12] is 97.60% based on majority voting on the individual classification results of all letters in a single page. Recent work [13] is based on convolutional neural networks (CNNs) which trains a group of three separate networks in parallel with inputs as “e”s, the median residual of “e”s and average residual of “e”s. Another group of three networks is trained with the above settings using letter “a”. Such a multi-classifier approach gives 97.33% page-level accuracy on the same data of [12]. If the input other than “e” and “a”, the results will not be very accurate.

2.1.1. Classification techniques

SVM [6] can classify pixels for images according to textural cues. It is a concept for classification, regression, and other learning tasks that can be simply explained as an attempt to find the best hyperplane which serves as a separator among classes in the input space. The best hyperplane separation among them can be found by measuring the margin hyperplane and looking for maximum points [22]. In addition, SVM is able to obtain the best result in comparison among feature extractions for a multi texture classification problem [23].

Other useful classifiers worth mentioning are Gaussian mixture model (GMM) and AdaBoost algorithm. Gaussian mixture model (GMM) [24] is a probabilistic model for representing normally distributed subpopulations within an overall population. Mixture models in general do not require knowing which subpopulation a data point belongs to, allowing the model to learn the subpopulations automatically. GMMs have been used for feature extraction from speech data, and have also

been used extensively in object tracking of multiple objects, where the number of mixture components and their means predict object locations at each frame in a video sequence. GMMs had been very successful in modeling speech features and in acoustic modeling for speech recognition for many years (until around year 2010–2011 when deep neural networks were shown to outperform the GMMs) [24].

The AdaBoost algorithm, which is one of the most popular boosting algorithms, generates a sequence of base models with different weight distributions over the training set [25]. It can be used in conjunction with many other types of learning algorithms to improve performance. The output of the other learning algorithms (“weak learners”) is combined into a weighted sum that represents the final output of the boosted classifier. AdaBoost is adaptive in the sense that subsequent weak learners are tweaked in favor of those instances misclassified by previous classifiers. AdaBoost is sensitive to noisy data and outliers. In some problems, it can be less susceptible to the overfitting problem than other learning algorithms. However, in [26,27], AdaBoost algorithm are not always expected to improve the performance of SVMs, and even they worsen the performance particularly. This fact is SVM is essentially a stable and strong classifier.

According to the literature survey and above mentioned analyses, the use of feature filters and SVM classification are the most commonly adopted solutions. From Table 1, the classifiers of the reported highest accurate rates for text or natural image documents are either from feature based SVM or CNN model of machine learning for source printer identification. Therefore, the experiments in this research focuses on using feature based SVM and CNN model of machine learning as the main classifiers.

Nevertheless, the use of feature sets are generally implemented independently based on the computation availability. As a consequence, the feature filter applicability of the underlying techniques involve experts and domain knowledge in order to explore the best feature sets and how to wisely select the most important features among large feature sets is still a critical issue. Therefore, those characters are generally handcrafted features which require sufficient training time.

Unlike feature based situation, deep learning technique allows the proposed model to learn the distribution and train the system automatically. Few human intervention is involved for the whole architecture for accurate identification rate which is technically inspiring for researchers to enhance the existing techniques and explore new forensics approaches.

2.2. The microscope used in this study

Since the common used scanner has the limit of the resolution, the microscopic images are applied in this study. The most suitable optical microscope to examine the printed document is the type of reflected light microscope with adjustable magnification. Fig. 1 illustrates the illumination technique of this microscope, the light path comes from the light source, moves into excitation filter, passes through the objective lens, then is reflected off the surface of the specimen, returns through the objective lens, and finally reaches the eyepiece or camera for observation. There are two magnification procedures in the reflected light microscope, i.e. optical magnification and digital magnification. The optical magnification is calculated from objective lens and subjective lens (ocular). For example, if 20 \times objective lens with 15 \times subjective lens will yield the 300 \times optical magnification. Furthermore, the digital magnification could be adjusted through the digital imaging processing and shown on the screen. In this study, the microscope OLYMPUS BX41 with the digital camera resolution 3.1 mega pixels and CCD Chip 2048 \times 1536 pixels is simulated [28].

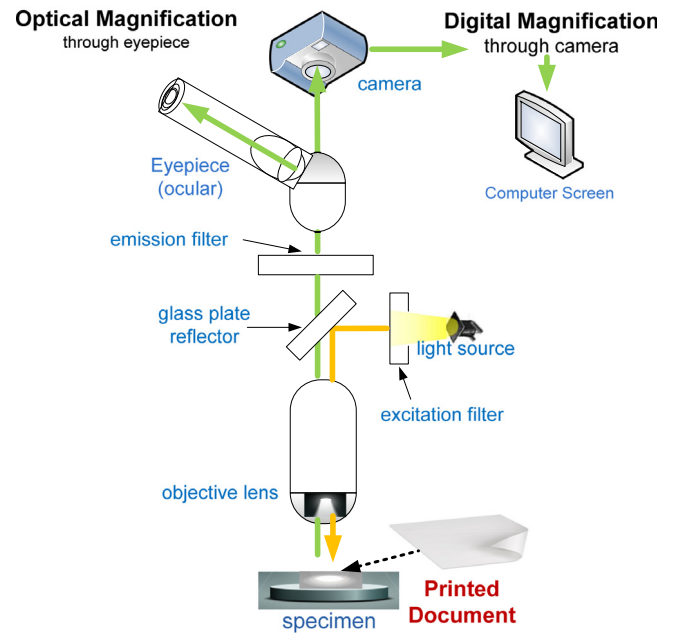


Fig. 1. The reflected light illumination of microscope.

2.3. Machine learning and deep learning

Machine learning is mainly about how the computer simulates and realizes human learning behavior, and allowing machine to do self-learning and acquire new knowledge or skills. Machine learning is also used in many different areas, such as: image recognition, voice recognition, natural language understanding, content recommendation, weather forecast and so on. The general procedures applying machine learning to solve the above mentioned problem is showed in Fig. 2. Reasoning, prediction or identification are the target for the machine learning. Data preprocessing, feature extraction and feature selection play key roles for machine learning. In the past, based on professional knowledge and experience, features are extracted heavily depending on human involvement. The process of manually feature selection is usually laborious and time consuming. Therefore, machine learning is a discipline that specializes in how computer simulates and realizes human learning behavior. If the technique can program computer to automatically learn the characteristics and speed up the whole procedures, it can save dramatic amount of time and money.

Accordingly, it is important to understand how the human brain works, and Hubel et al. [29] had found that the operation of the neuron system is hierarchical based on the functional analysis of the cortex cells of the cat to find the corresponding relationship between neurons. Under such understanding, the integration of artificial neural network and the back propagation facilitate the analysis of a large number of input training samples to get the statistical regularity, and to make the prediction.

More advanced machine learning system called the deep learning has used more hidden layers of artificial neural network as shown in Fig. 3, to achieve the multi-layer operation of the neural system. The basic concept is the output of the previous layer as the input of the next layer and the input information can be hierarchically expressed by combining the low-level features to form more high-level abstract features.

Hinton et al. [30] have reported that the multi-hidden artificial neural network has excellent learning capability. The learned features are conducive to visualization and classification. In addition, deep



Fig. 2. The learning procedures of machine learning.

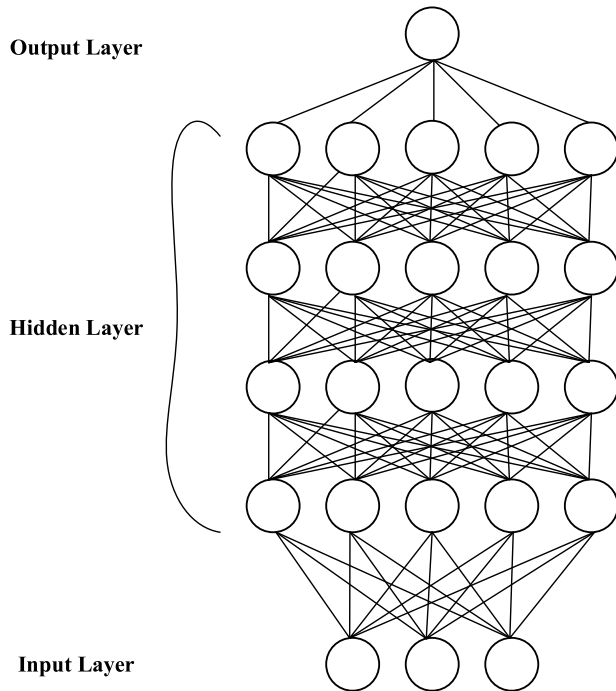


Fig. 3. The multi hidden layer structure of deep learning model.

neural networks can overcome the difficulty of training through “layer-wise pre-training”. Consequently, deep learning can establish a multi-hidden layer of learning model to process a large number of training samples, learn useful features and enhance the classification or prediction accuracy. Deep learning has also developed many different models such as: Auto Encoder, Sparse Coding, Restricted Boltzmann Machine (RBM) [31], Deep Belief Networks and Convolutional Neural Networks (CNN). Related studies have achieved great success in many fields of human machine interaction [32].

2.3.1. Convolutional neural networks (CNNs)

Convolutional neural networks (CNNs) is a type of artificial neural network that was proposed by Lecun et al. [32] it has become one of the popular tools in the field of speech analysis and image recognition. Its shared weights network structure is very similar to the actual biological neural network in simulation. This feature can also reduce the complexity of network model and reduce the number of parameters. CNNs can directly use the image as the input which can avoid the traditional identification method by complex feature extraction and data reconstruction. The network structure of a convolutional neural network is highly invariant for image translation, scaling up/down, tilting or other forms of deformation.

The neurons in the convoluted neural network are derived from the concept of receptive field proposed by Hubel et al. [29] through the study of cat visual cortical cells, followed by Japanese scholar Kunihiko Fukushima. Based on the concept of receptive field, the neocognition can be regarded as the first realization network of the convolutional neural network and the first application of the field in the artificial neural network. The neural cognition machine usually contains two

types of neurons: the S-element of the characteristic extraction and the anti-deformation C-element. There are two important parameters in the S-element: the field and the threshold parameter, the former determines the number of input connections, the latter controls the degree of response to the characteristic sub-mode. Thereafter, the neural cognitive machine has more different development, convoluted neural network can be seen as a form of neural cognitive promotion, and neural cognitive machine is a special case of convolution neural network.

Convolution neural network [8] is a multi-layer neural network that each layer consists of multiple two-dimensional planes. This plane is composed of multiple independent neurons, the basic concept of network architecture as shown in Fig. 4. The C layer in the graph is the feature extraction layer, and the input of each neuron connects with the local receptive field of the previous layer, and the local feature is extracted. When the local feature is extracted, its positional relationship with other features will also be determined. The S layer in the graph is the feature mapping layer, and each feature layer of the network is composed of multiple feature mapping layers. Each feature is mapped to a plane, and the weights of all the neurons on the plane are equal. The feature mapping structure adopts the influence function kernel, the small sigmoid function acts as the activation function of the convolution network, so that the feature map has the displacement invariance. In addition, since neurons on a map surface share weights, it is possible to reduce the number of network parameters and reduce the complexity of network parameter selection. Each feature extraction layer (C layer) in the convolutional neural network is followed by a computational layer (S layer) for local averaging and secondary extraction.

Convolution neural network consists of five basic network layers: input layer, convolutional layer, rectified linear unit (ReLU), pooling layers, and fully connected layer:

- (1) Input Layer:
The entrance for the input data.
- (2) Convolutional Layers:
This layer contains a series of fixed-size filters, which are used to operate the convolution of the input data, resulting in the so-called eigenvalue map (feature map). These filters can provide useful modules for image recognition, such as image edges, regular patterns, and color changes. The amount to be used depends on the size of the data, the complexity of the image, and the size of the image. There are two important settings, Padding is set to determine how many columns around the image to increase or how many rows of null pixels added; and Stride is set in the filter about how many pixels to move during the scan. These two parameters determine how the filter can scan the full image
- (3) Rectified Linear Unit (ReLU):
ReLU generally follows the operation of the convolutional layer and provides the output with the non-saturating activation function $f(x) = \max(0, x)$. According to Krizhevsky’s study [8], these equations can be used in convolution of neural networks in the rapid convergence of training, also dealing with the elimination of gradient problems to speed up the training.
- (4) Pooling Layers:
The pooling layer is to reduce the spatial size of the representation and the number of parameters. It also minimizes the computation number through the feature map and controls overfitting. The pooling operation arrange several form of translation invariance and sporadically insert the pooling layers among successive convolutional layers in the CNN architecture. Therefore, the network can focus only on the important modules generated by convolutional layers.

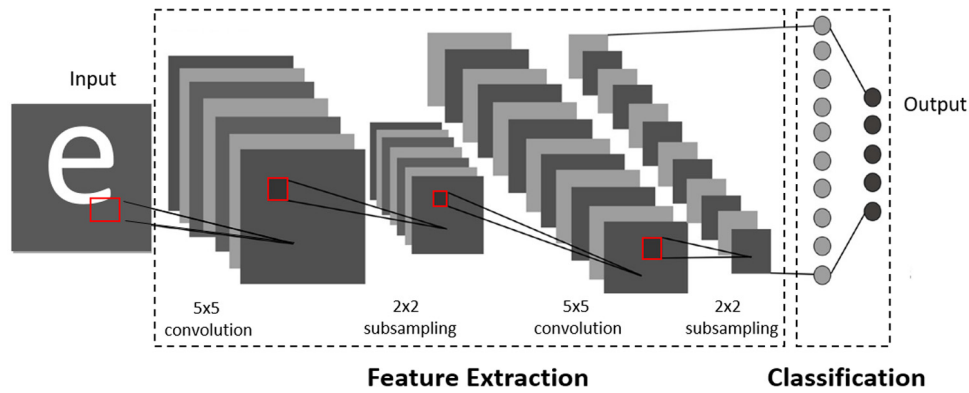


Fig. 4. The network architecture of CNNs.

(5) Fully-connected Layers

This layer locates at the very end of the entire network and plays the role of a classifier, often accompanied by the soft-max classifier to make the classification decision of the input.

In the convolutional neural network [33], the type of the network layer is arranged according to the different application objectives. The convolution layer, ReLU, the pooling layer forms a core unit. According to the different contents of the input data, the parameters will be adjusted in order to establish a neural network that meets the requirements of the system.

The training of convolutional neural network is mainly operated through the back propagation algorithm and stochastic gradient descent with momentum algorithm. Back propagation can be divided into two phases: propagation and weight update. It technically calculates the gradient of the loss function, and then feedback to the optimization method for weight update [34]. Compared to the standard gradient descent method using the entire dataset, the stochastic gradient descent method for each period of interaction uses the training subset called mini-batch. It minimizes the error function by updating parameters of weight and bias, and the parameter updating is calculated by the gradient of the loss function fed back by the Back Propagation [34].

2.4. Feature filter based SVM classification

Since feature filter based SVM classification is widely applied in many classification schemes as shown in Table 1 and the features are important characteristics extracted from the printed documents, brief explanation of those filters adopted in this study is introduced in the following:

2.4.1. The spatial features

Gray-Level Co-Occurrence Matrix (GLCM) features [19] are the estimates of the second order probability density function of the pixels in the image where the overall spatial relationships are calculated. GLCM is a statistical method of examining texture that considers the spatial relationship of pixels. The GLCM statistical function characterizes the texture of an image by calculating how often pairs of pixel with specific values and in a specified spatial relationship occur in an image, and then extracting statistical measures from this matrix.

The other spatial features [5] are Discrete Wavelet Transform (DWT) [10], Gaussian, Laplacian of Gaussian (LoG), Unsharp, Wiener, and Gabor [28].

The DWT feature set in this study focused on a two-dimensional scaling wavelet that is a product of two one-dimensional functions based on the research of [28]. There are four subbands which are subsampled as decomposed image shown in Fig. 5. The sub-bands can give a label LH₁, HL₁ and HH₁ and the detailed image LL₁ corresponds to the coarse level coefficients such as an approximation image. However, the sub-band LL₁ is critical sampled after decomposing. This process

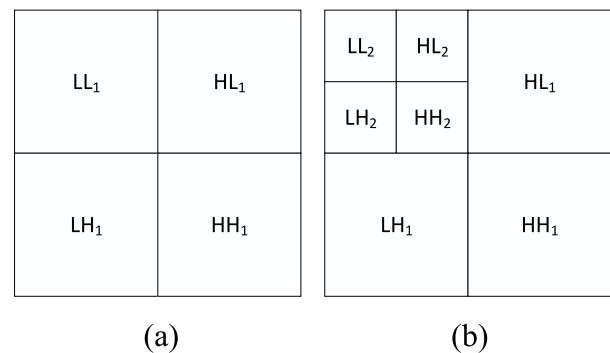


Fig. 5. DWT Image decomposition (a) One-level (b) two levels.

is a two-level wavelet decomposition and can be further decomposed by using LL₂ until the final scaled decomposition is accomplished. By using this filter set, there are 12 statistical features which include standard deviation, skewness, and kurtosis for four HH, LH, HL, LL sub-bands [10,28].

Gaussian filter can minimize the image noise based on probability distribution function [29] after the process of convolution. Gabor filter is a two-dimensional filter which has the Gaussian kernel function modulated by a complex sinusoidal plane wave and has several advantages such as invariance to illumination, rotation, scale, and translation [5]. In the spatial and the spatial-frequency domain, it is a set of orientation and frequency sensitive band pass filters which have the optimum joint resolution. The setting involves: wavelength specifies the wavelength of the cosine factor of the Gabor function. Orientation specifies the orientation of the normal to the parallel stripes of the Gabor function. Phase offset specifies the phase offset of the cosine factor of the Gabor function. Aspect ratio specifies the ellipticity of the Gaussian factor. Bandwidth specifies the spatial-frequency bandwidth of the filter when the Gabor function is used as a filter kernel. This study implemented the Gabor orientation for scanned image upon four values, i.e. 0°, 45°, 90° and 135°. The variance s_x along x and s_y along y axis, f is the frequency of sinusoidal function and θ is the orientation of Gabor function. The settings of $s_x = 4, s_y = 12, f = 4, 12, 24, 48, \theta = 0, \pi/4, \pi/2, \text{ and } 3\pi/4$ yield 48 different feature filters for feature extraction [28]

Additionally, the co-occurrence matrix and texture features are the most popular second-order statistical features which are introduced by RM Haralick in 1973 [35] also used in this study.

2.4.2. The fractal and LBP feature filters

In this study, we extracted fractal based features by calculating the fractal dimension (Segmentation-based fractal analysis SFTA) [36]. These features are built on fractal dimension for gray-scale images which depict objects and structure boundary. LBP is a feature extractor that

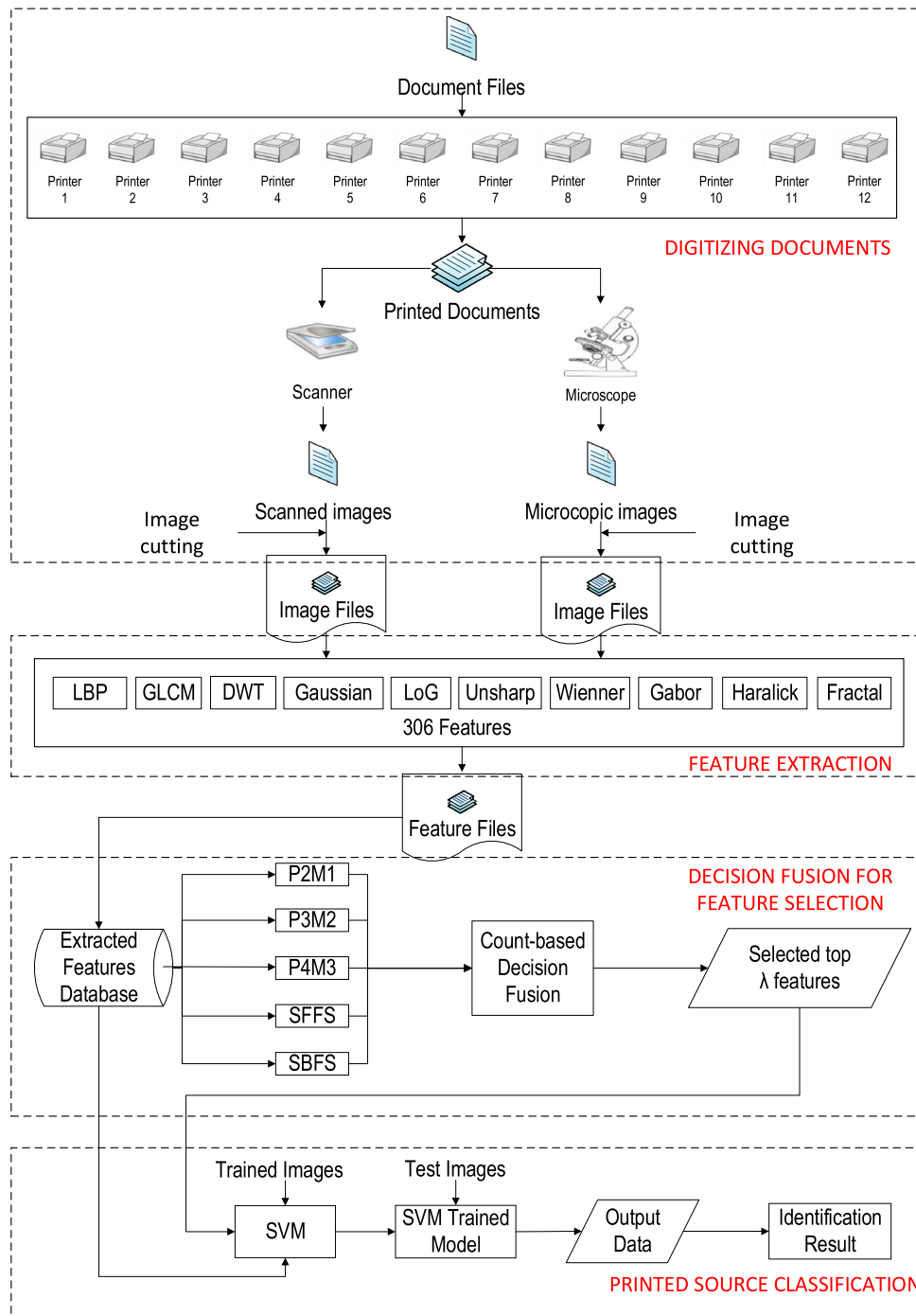


Fig. 6. The flowchart of feature based SVM system.

has an appropriate and powerful sub pattern-based texture descriptor. It characterizes the gray-scale invariant texture and combination between measuring texture from each neighborhood and the difference of the average gray level of those pixels based on binary numbers [37].

2.4.3. Decision fusion approach

The decision fusion model referring to the feature-selection and decision fusion technique is therefore explored. The floating search methods are implemented by the sequential selection procedures that are related to the *plus l take-away r* algorithms [38]. Plus *l* minus *r* selection (LRS) starts from the empty set and repeatedly adds *l* features and removes *r* features when *l* is more than *r*. Conversely, when *l* is less than *r*, LRS starts from the full set and repetitively removes *r* features

followed by *l* additions. It can be implemented by using plus 2 minus 1 (P2M1) where ($l = 2, r = 1$), plus 3 minus 2 (P3M2) where ($l = 3, r = 2$), and plus 4 minus 3 (P4M3) where ($l = 4, r = 3$). Furthermore, to perform feature selection, Pudil et al. [39] proposed the SFFS and SBFS methods. The SFFS method is a modified plus-*m*-minus-*r* by one more mechanism in the minus step. The SFFS method can be described algorithmically in a similar way to the previous method.

A challenge of feature selection integration or fusion represents the method of combining the above mentioned five different techniques of feature selection (P2M1, P3M2, P4M3, SFFS, and SBFS). The goal here is to gather the most useful features from all the selection methods, in such a way that the end-result is to achieve the maximum outcomes

from each technique respectively and then making a fusion from each of them after aggregation.

3. The research method

This study will use two different identification systems: the statistical feature based classification method by SVM, and the other one developed by convolutional neural network based classification. The text and image documents will be examined either scanned by scanner or microscope.

Both methods will be explained as following:

3.1. Feature based SVM classification

The diagram shown in Fig. 6 illustrates the identifying procedures for feature based classification which can be divided into five stages such as, printing documents, digitizing documents, feature extraction, feature selection, and classification:

- (1) *Printing documents*: First of all, text and image documents are prepared. For example, different font-type with different font size for characters are studied. In this paper, several printed characters are identified such as commonly used English character “e”, Chinese character “永”, Arabic character “ع”, and Japanese character “え”. We also investigated the image documents (i.e. Lena, Peppers, Baboon and Wikipedia images) for comparison. Next, all the documents are printed by using 12 printers where brands and models are shown in Table 2.
- (2) *Digitizing documents*: After all the documents have been printed, the second step is to digitize document either by using a scanner or a microscope. At this stage, the text document types are recognized as either text or image document. If the document is identified as text file, region of interest for the extracted characters will be further labeled to remove the blank space in order to obtain the most valuable scanned information.
- (3) *Feature extraction*: Extracting the grayscale documents by the proposed filters such as LBP, GLCM, DWT, Gaussian, LoG, Unsharp, Wiener, Gabor, Haralick, and fractal filters. Each character or images are extracted by using ten different feature sets based on the printer sources. For example, the character “e” that originates from each type of printer, we extracted at least 1200 images for each printer by using different feature filters into numeric values. In this study, there are total 306 statistical features which is a very large feature space compared with features adopted in [9–20]. Therefore, the computational complexity is also a critical issue to be resolved in real applications. Therefore, feature selection will be conducted in the next stage to alleviate the computation demands.
- (4) *Feature selection and fusion*: The adaptive feature selection algorithm is implemented here in order to find the most important λ features which helps to reduce the total evaluation time without the loss of accuracy. Five feature selection algorithms P2M1, P3M2, P4M3, SFFS, and SBFS are adopted for the feature selection processes [10]. The count-based aggregation is utilized at decision fusion stage where each feature will get a recommending label whenever a feature is chosen into the optimal subset by a selecting algorithm. Based on the majority vote, the features with the most labels are selected into the final optimal subset which will be used for classification.
- (5) *Printer classification*: The last step of the source identification is to classify the printed sources from different printers using the optimal features from step (4) by using SVM trained model. The extracted images that have been in the numeric value are then inserted into MySQL database. The database contains different schema and query based on printed document type which will be evaluated. Afterwards, this study classifies them by using SVM in the Java environment (Eclipse Indigo) and same SVM parameters applied in [6,9–12] are adopted here.

The steps of proposed approaches are listed below:

Table 2
Printer brand and models used in this study.

No.	Brand	Model
1	HP	CP3525dn
2	HP	DesignJet 111
3	HP	LaserJet 300 Color
4	HP	LaserJet 600 M603
5	HP	ColorLaserJet3800dn
6	HP	LaserJet 3055
7	HP	LaserJet 4100
8	HP	LaserJet P2055dn
9	HP	LaserJet P3015
10	HP	LaserJet 4350n
11	Fuji	C2200
12	Sharp	MX 2010U

1. 10 sets of images from the image database of 12 printer sources are randomly generated. In each set, there are 500 images which are selected from each printer as training data and another 300 images for test data. 10 sets of feature filters are then applied for characteristic extraction.
2. Apply the SVM engine to build the prediction models using 10 sets of feature filter.
3. Feed the test image subsets to the corresponding model trained in step 2 for the printer source prediction.
4. Repeat step 1 through 3 ten times to obtain the predicted results.

3.2. Deep learning based classification

The procedure is shown in Fig. 7 with the following steps:

- (1) Same as the procedure of 3.1(1) printing documents and 3.1(2) digitizing documents.
- (2) Feature extraction and feature selection and classification are all substituted by the convolutional neural network. The different combination of convolutional layer, ReLU layer and pooling layer form a multi-layer neural network. Apply the system to train samples, automatically learn the characteristics of the images from different printers. The fully-connected layer with soft-max operation play the role of classifier.

Based on the above steps, the successful design of the layer architecture of CNNs is the core of the identification system to achieve high accuracy rate. The design of the network layer and the parameters are described as following:

- (1) *Input layer*: the network layer reads the training samples and generates output to the convolutional layer. Since scanned images and microscopic grayscale images have different pixel dimension, we adjust the dimensionality of the input sample based on the size of the image. For example, the scanned image dimension is 51×51 pixels, and the microscopic grayscale images are 45×45 pixels and 90×90 pixels respectively.
- (2) *Convolutional layers*: a series of filters are used to convolve the images from the input layer and generate the feature map through convolutional layer. This study will apply three convolutional layers, each of the filter size of convolutional layers is 5×5 , zero-padding is set to 2, and stride is set to 1. The first and second convolutional layers use 32 filters to scan the image, and the third convolutional layer uses 64 filters.
- (3) *ReLU layers*: each convolutional layer is generally followed by the ReLU layer which primarily helps the training to converge quickly and avoids overfitting. The standard non-linear equation $f(x) = \max(0, x)$ is used in the experiments.

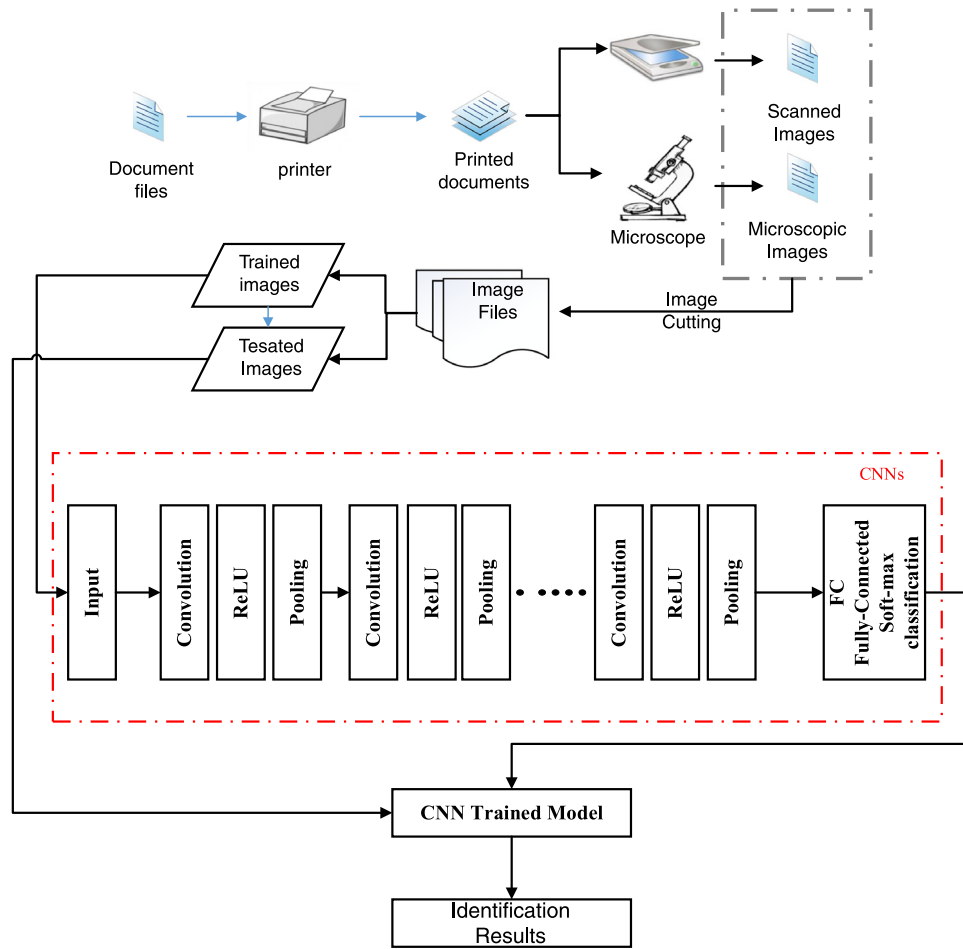


Fig. 7. The flowchart of CNNs system.

- (4) Pooling layers: a pooling layer reduces the dimensions of the images for subsequent network layers. Each pooling layer has a window dimension of 2×2 , and stride is set to 2. It means that the window scans the image and moves two pixels right and down each time. The first and second pooling layers use the max-pooling and the last one uses average-pooling.
- (5) Fully-connected Layers: only one fully-connected layer is used in the experiments with a soft-max layer and a classification layer to classify the image source of the printer. Since 12 printers are used, the parameter settings of the category is 12.

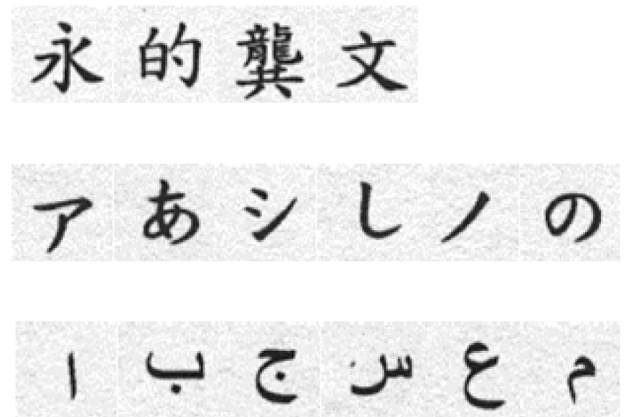


Fig. 8. The character samples used in the experiments.

The rest of the network architecture is set as follows: the initial learning rate of neural network is 0.001. After every 10 cycles of training, the rate will be reduced by 90%. Each experiment will perform 30 cycles of training and each training will process 100 images. Each training sample is randomly selected and each trained image is labeled which will not be selected as testing.

Table 3 summarizes the network layer design of the overall CNNs architecture, where “CONV + POOLmax” represents the convolutional layer and followed by the use of the maximum generalized pooling layer. The “CONV + POOLavg” is followed by the use of pooling layer of average generalization.

4. Experiments and discussion

In this study, text and images are used for the simulation. Some commonly used word characters for English, Chinese, Arabic and Japanese are applied, as well as benchmarked image like Lena, Peppers and Baboon. The text and image samples are illustrated in Figs. 8–9. For the experiments, 12 printers are used and details are tabulated in Table 2.

For each printer, 1200 samples are extracted from the scanned image for each character.

4.1. Data samples

The study of printed document is categorized into text and image documents. To validate and compare the document, the samples are distinguished not only for text document with different language scripts but also for image document with different samples. For text document, the text includes English character “e”, Chinese character “永”, Arabic

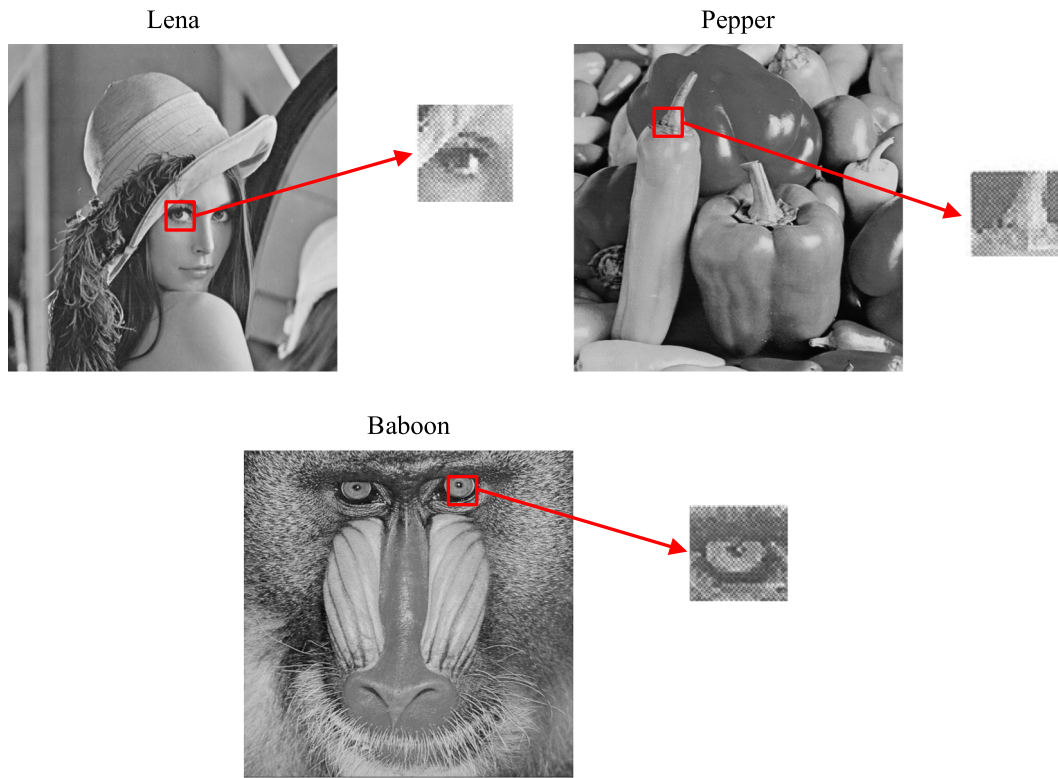


Fig. 9. The scanned image samples used in the experiments for Lena, Peppers and Baboon.

Table 3
Summary of parameters for CNNs.

Layers	1	2	3	4
Type	CONV + POOL _{max}	CONV + POOL _{max}	CONV + POOL _{avg}	FC
Filter numbers	32	32	64	12
Filter size	5 × 5	5 × 5	5 × 5	–
Convolution stride	1 × 1	1 × 1	1 × 1	–
Pooling size	2 × 2	2 × 2	2 × 2	–
Pooling stride	2 × 2	2 × 2	2 × 2	–
Padding size	2 × 2	2 × 2	2 × 2	–

character “ㄟ”, and Japanese character “ㄟ”, some samples are illustrates in Fig. 8. There are different reasons to select those characters. For example, English character “e” is widely analyzed from various literatures [10,20]. On the other hand, each stroke of Chinese character “永” represents the basic strokes for Chinese calligraphy [10]. Arabic character “ㄟ” and Japanese character “ㄟ” are selected since both characters are with few number of strokes in its language category. Since the scanned images and microscopic images will be evaluated, the detailed data sample will be explained respectively.

4.1.1. Scanned image

All the scanned text images are scanned by BenQ 3300U and the resolution is 300dpi. After digitizing the document, the 10pt text images are cropped by using software Netbean IDE 8.0 with the pixel size 51 × 51 and the file size is 3.64 kilobytes for each character. At least 1200 image samples are examined for each character from one printer source. Hence, the number of sample in each text document is at least 14,400 images from 12 printers.

For image document, only part of the image extracted from Lena, Peppers and Baboon are used as shown in Fig. 9. The dimension size of each image patch is also 51 × 51 with 3.64 kilobyte. Each image will be extracted at least 1200 image patch samples from each printer. Thus, the total number of samples for each image document is at least 14,400 images from 12 printers.

4.1.2. Microscopic image

A reflected microscope Olympus CX41 with 300× magnification is applied in this study. All microscopic images for the text documents are in JPG file format with the dimension of 1600 × 1200 and file size 2.73 KB. Next, all the images are converted into grayscale in bitmap file format (BMP). After digitizing the documents, the images are cropped by using software Netbean IDE 8.0. Fig. 10 shows the cropping method for the acquired image patches of the text document “永”, with pixel size 45 × 45 in each microscopic image. To augment the learning capability of machine learning, overlapped images for size 90 × 90 are also obtained as shown in Fig. 10(b).

4.2. Experiments

4.2.1. Experiment I: Comparison of different CNNs network architecture

While establishing a deep neural network, the structure will be designed according to the amount of data and the complexity of the image content. It is not necessary that more hidden layers included will accomplish higher accuracy results due to the overfitting in the network. The design principle is not only to get a concise network architecture for less training time but also to achieve high accuracy rate.

In this experiment, the network architecture has three different depth, either using 1, 2 or 3 convolutional layers respectively, and each convolutional layer will be equipped with ReLU layer and pooling layer. Therefore, total 7 layer, 10 layer and 13 layer neural network models are design for comparison. The text image inputs include characters for Chinese, Japanese, Arabic, and images including Lena, Peppers and Baboon. There are 500 training samples from the images in each category for training and randomly selected 300 samples from the remaining images as test samples. Each text and image of the experimental samples are sent to the 7, 10 and 13 layer CNNs network (details in Table 3) for training, classified respectively and the results are shown in Tables 4–7.

According to Table 4, the highest accuracy rate for 1 conv CNNs is 98.99% for Chinese character “永” and the lowest one is 93.34% for “文”. In Table 5, the highest accuracy rate for Japanese character

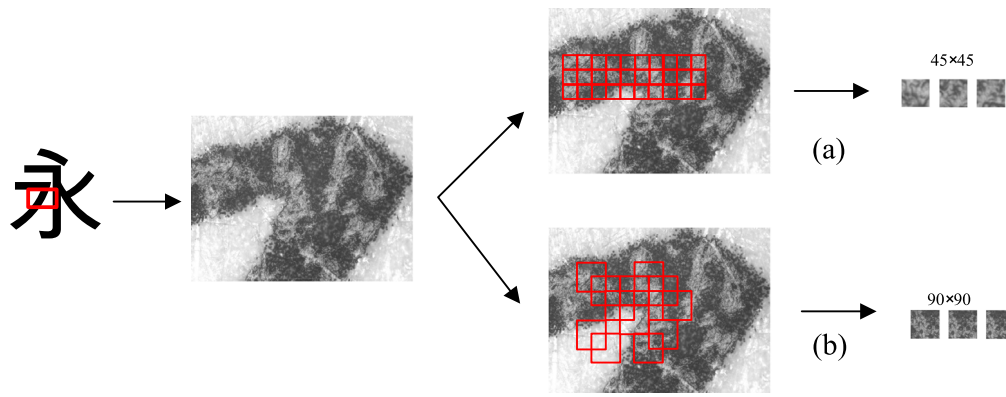


Fig. 10. “永” captured microscopic images for character (a) patch image with 45 × 45 pixel size (b) overlapping patch image with 90 × 90 pixel size.

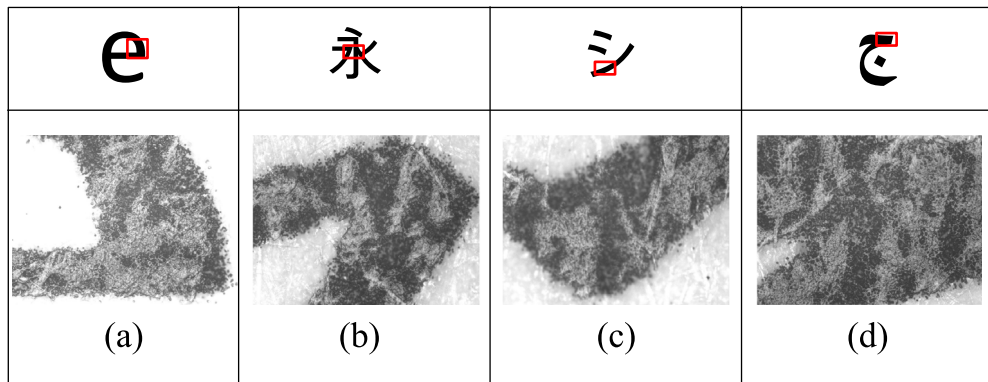


Fig. 11. Sample microscopic images for characters (a) is English character “e”, (b) is Chinese character “永”, (c) is Japanese character “シ” and (d) is Arabic character “ع”.

Table 4
The accuracy rates for Chinese characters.

	永	龔	的	文
1 conv (7 Layers)	98.99%	97.09%	98.24%	93.34%
2 conv (10 Layers)	98.19%	95.57%	97.33%	90.29%
3 conv (13 Layers)	91.33%	88.62%	93.38%	79.71%

Table 5
The accuracy rates for Japanese characters.

	ア	あ	シ	し	ノ	の
1 conv (7 Layers)	98.44%	99.01%	99.21%	98.99%	98.21%	99.02%
2 conv (10 Layers)	95.89%	96.98%	96.09%	96.11%	96.32%	96.12%
3 conv (13 Layers)	83.54%	80.12%	82.23%	84.76%	84.12%	83.69%

Table 6
The accuracy rates for Arabic characters.

	ا	ب	ج	س	ع	م
1 conv (7 Layers)	98.78%	98.96%	99.36%	99.22%	98.77%	98.94%
2 conv (10 Layers)	98.65%	98.21%	98.96%	98.50%	97.89%	97.98%
3 conv (13 Layers)	89.21%	87.82%	88.03%	94.61%	89.03%	89.25%

is “シ” at 99.21% and the lowest one is 98.21% for “ノ” for 1 conv CNNs. According to Table 6, the highest recognition rate for Arabic

Table 7
The accuracy rates for images.

	Lena	Peppers	Baboon
1 conv (7 Layers)	99.95%	99.92%	99.93%
2 conv (10 Layers)	99.88%	99.89%	99.90%
3 conv (13 Layers)	99.75%	99.82%	99.91%

character is 99.36% of “ع” and the lowest one is 98.77% for “ع” for 1 conv CNNs. From above observation, the amount of strokes in text data has significant influence during the classification while the character with less strokes is much harder for classification. In addition, deeper CNNs structure with more than one convolution does not improve the accuracy rates for the classification when input data is text. However, the accuracy rates for different CNNs systems are extremely high for image Lena, Peppers and Baboon in Table 7. Unlike the text input, the natural images with complicated content provides more information for the neural networks and there is no overfitting situation for deeper CNNs. From the experimental data in Tables 4–7, it is clear that 7 layers CNNs can achieve the highest accuracy rate for of the text and natural image data.

4.2.2. Experiment II: Comparison of feature based SVM classification system and CNNs based classification system for scanned data

It is an interesting topic to discover the performance behavior between the feature based SVM classification system and CNNs based classification system. Previous studies [10–12] have proposed feature selection and decision fusion technique for printer source identification. In Section 4.2.1, different depth structure of CNNs has been simulated and the developed architecture will be implemented here for comparison.

The procedures from Section 3.1 will be implemented and Arabic character “ع” will be trained for the featured based SVM system. Since

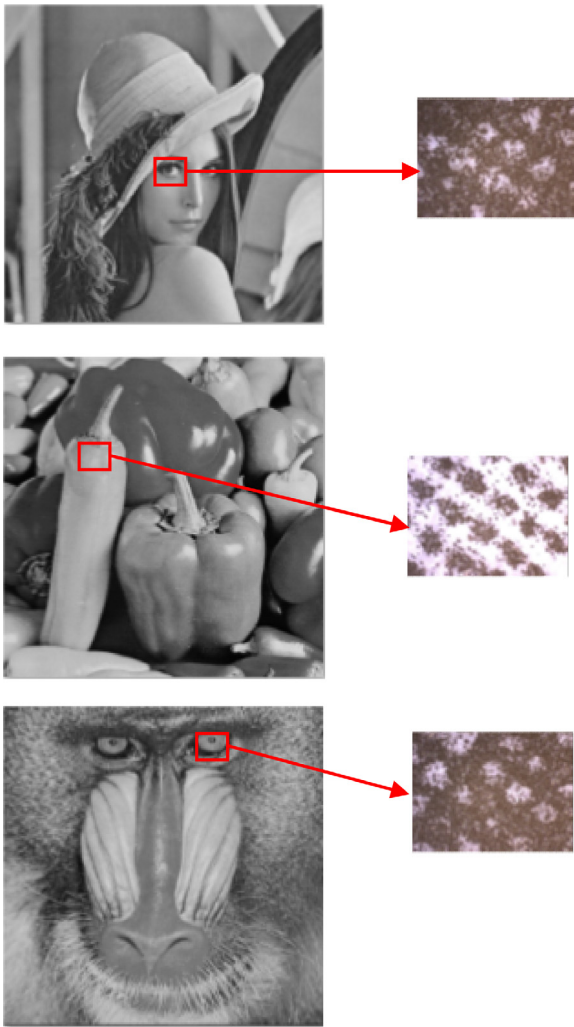


Fig. 12. “□” captured microscopic images for Lena, Peppers and Baboon.

Table 8
Comparison of feature based SVM classification system and CNNs based classification system for scanned images.

	永	シ	ع	Lena	Pepper	Baboon
SVM (306 features)	98.46%	96.11%	98.77%	99.84%	99.89%	99.89%
SVM (222 features)	99.23%	97.50%	99.43%	99.93%	99.97%	99.94%
1 conv (7 Layers)	98.99%	99.21%	99.36%	99.95%	99.92%	99.93%
2 conv (10 Layers)	98.19%	96.09%	98.96%	99.88%	99.89%	99.90%
3 conv (13 Layers)	91.33%	82.23%	88.03%	99.75%	99.82%	99.91%

the total number of feature is 306, the number of selected feature will be reduced to 222 according to the experiment. The trained system will perform the printer source classification for Chinese character “永”, Japanese character “シ”, Arabic character “ع”, Lena, Peppers and Baboon images respectively and the results are tabulated in Table 8. Since the feature based SVM system is optimized for Arabic character “ع”, there is no doubt that the accuracy rates for “ع” are the best among characters using the handcrafted features.

After closely examining the experimental results in Table 8 for text and image input, the identification rates by deep learning based forensic approach can achieve comparable results compared to the technique by

SVM with feature selections [10]. Surprisingly, the accuracy rate for Japanese character “シ” achieves higher rate than SVM approach with feature selection in Table 8. In most cases, 1 conv CNNs structure based deep learning system can achieve high accuracy results for both text and image documents while the input is from scanned images. This suggests that it is promising that deep learning based method can even achieve better results than handcrafted mechanism.

4.2.3. Experiment III: deep learning based system for microscopic images

According to Ferreira et al. [13], they suggested that using an optical microscope to obtain the grayscale image of a printed document could improve the accuracy rate for classification. Tsai et al. [28] had successfully applied feature based SVM identification system to achieve high accuracy rates for text and images obtained by optical microscope. It is very interesting to see whether CNNs based system can get similar results as the analyses in Section 4.2.2 or not.

In this experiment, the characters and images used in Experiment two are included and the English character “e” is also added as the training samples. Due to high magnification capability of the optical microscope, the field of view is limited to a certain area of the character and images which cannot cover the entire character or entire image. Figs. 11 and 12 illustrates the local region which will be examined in this experiment.

To observe and compare the text from different printers and different alphabets, character “e” (English), character “ع” (Arabic), character “シ” (Japanese) and character “永” (Chinese) are examined. The characters are taken from the same microscope with the same magnification. As shown in Fig. 11, the microscopic images printed from Printer HP Color LaserJet CP3525 are illustrated for comparison. Fig. 11(a) is English character “e”, Fig. 11(b) is Chinese character “永”, Fig. 11(c) is Japanese character “シ” and Fig. 11(d) is Arabic character “ع”. The printed characters are from the same printer and the particle shape such as bubbles and dots are clearly grouped to form the letters.

Similarly, Lena, Peppers, and Baboon images are also tested. Unlike the alphabets, the region of interest in the images is universally important across the image. Therefore, a given region for each image is selected as shown in Fig. 12. Since each image generated by the microscope has 1600×1200 pixels, the microscopic image is equally divided into a number of patches that represent the texture from specific printer sources. There are two type of patches as the input image for CNNs system, one type patch is 45×45 pixels without overlapping, and the other one is 90×90 pixels with overlapping as shown in Fig. 10. The use of overlapping is to enlarge the image size by 45 pixels for each patch which will augment the patch data with more texture information included. Fig. 13 illustrates the patch images at one location for 12 printers of printed Chinese character “永”. Statistically speaking, at least 1200 microscopic image patches will be extracted for either text or image document respectively for each printer.

The network structure used in Experiment III is similar to the structure in Experiment I either with 7 layers, 10 layers or 13 layers. Non overlapping patches and overlapping patches will be trained respectively for the system. Similarly, 500 samples are randomly selected from the data set for training to create the network model. From the remaining data, 300 images are randomly selected for testing. The identification results are tabulated in Table 9 for 45×45 patch and Table 10 for 90×90 patch. According to the results of this experiment, the identification rates increase while the network layer increases in Table 9 for 45×45 patch type. It is apparent that 13 layers of neural network with 3 convolution will achieve the best results with higher complexity. However, the accuracy rates for characters are quite low for microscopic image input and the results for natural image input are also poor for Lena, Pepper and Baboon.

For 90×90 overlapping patch type, the results in Table 10 are generally superior to the results in Table 9 since the augmented information by overlapping improves the classification capability while the network layer increases. In the mean time, the best classification

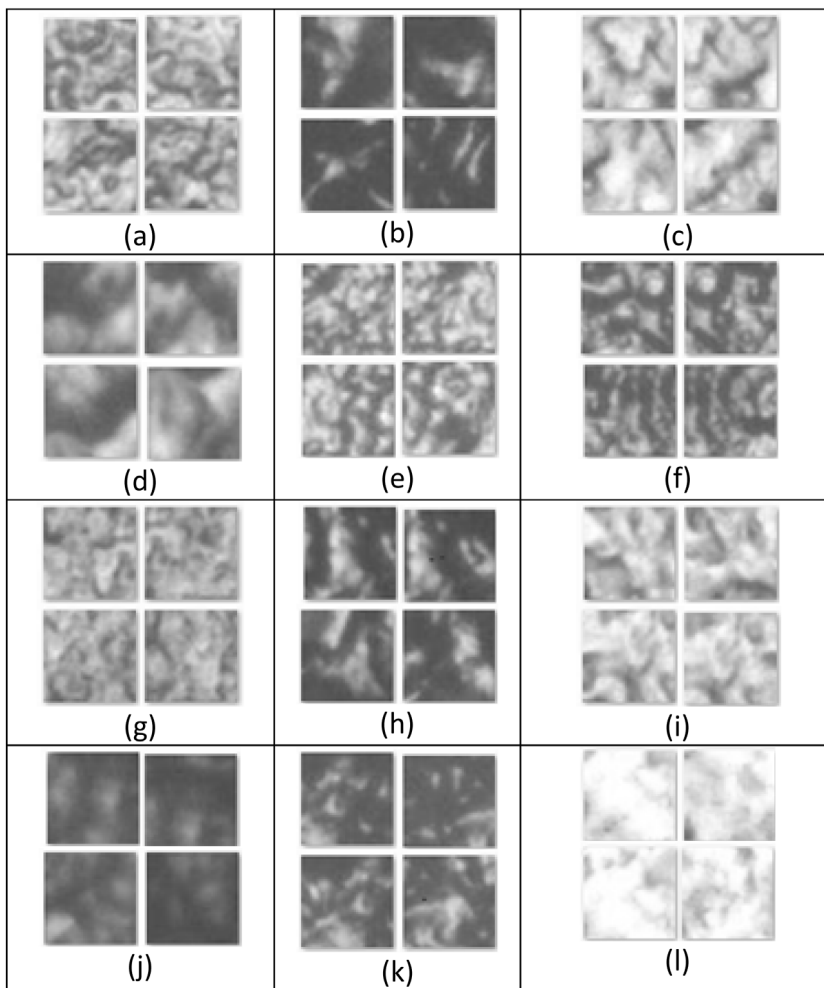


Fig. 13. Image samples for Chinese character “永” from 12 different printers in 45×45 pixel size.

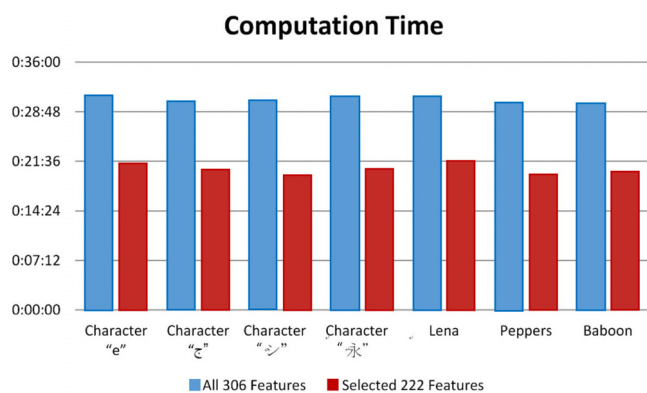


Fig. 14. Computation time for printer classification.

results based on SVM feature selection [28] is shown in Table 11 for the same experiment of 45×45 patch while text and natural image are applied. Apparently, the results of feature based SVM classification achieve higher accuracy rates than the results of Tables 9 and 10 based on deep learning approach.

Since image texture obtained by optical microscope are not structurally defined due to limited field of view as shown in Fig. 11, larger patch size can improve the extraction of image features through layers of abstraction for system in order to achieve better classification outcomes.

Table 9

The accuracy rates for microscopic image input with 45×45 pixel patch.

45×45 pixels	e	永	シ	ㄗ	Lena	Pepper	Baboon
1 conv (7 Layers)	49.35%	57.79%	60.90%	62.39%	50.11%	54.01%	68.48%
2 conv (10 Layers)	68.46%	87.09%	94.21%	94.20%	87.76%	91.39%	96.89%
3 conv (13 Layers)	68.49%	88.13%	93.17%	89.21%	92.14%	96.06%	97.01%

Table 10

The accuracy rates for microscopic image input with 90×90 pixel patch.

90×90 pixels	e	永	シ	ㄗ	Lena	Pepper	Baboon
1 conv (7 Layers)	69.21%	75.56%	69.24%	68.22%	67.89%	63.90%	69.80%
2 conv (10 Layers)	97.38%	96.68%	97.67%	90.20%	96.69%	95.44%	97.56%
3 conv (13 Layers)	98.01%	96.81%	97.78%	96.91%	97.01%	98.20%	97.89%

In addition, the success of machine learning generally requires big data support, the researchers suspect that the reason of inferior performance by deep learning is due to the constraints of data size in forensic identification. Currently, the experimental condition requires 1200 samples, 500 for training and 300 for testing. Under the same constraints of data

Table 11
The classification accuracy for 45×45 image patch using feature based classification [28].

e	永	シ	こ	Lena	Pepper	Baboon
99.95%	99.97%	99.98%	99.95%	99.97%	99.99%	99.99%

Table 12
Comparison of computation time for Japanese character “あ” by different layer’s CNNs.

	1 conv 7 layers	2 conv 10 layers	3 conv 13 layers
Training time	2436 s	3915 s	4588 s
Classification rate (Testing time)	99.01% (17.727 s)	96.68% (20.315 s)	80.12% (22.428 s)

size, feature based SVM classification could apply the known statistical filter to extract the important features for classification, deep learning still need extra amount of input to train the model successfully. To improve the accuracy performance, larger data size may be needed in order to train the deep learning model well.

4.3. Discussion

Currently, there are no standard benchmark tests of digital forensics for printer source identification. To make a fair comparison, the same experimental procedure and requirement are performed in this study based on the pioneer work of [9]. Since the computation cost is basically based on the image size, the time requirement is similar for scanned images and microscopic images. Therefore, only the computation of scanned image is discussed here such that other situation could be derived easily. The performance comparisons for the simulation are shown in Fig. 14 and Table 12 respectively. The analyses can be categorized into two areas: computation and accuracy issues.

• Computation analysis

Fig. 14 illustrates the line graph for the classification computation time required in scanned image for different characters and images by feature based SVM system. The time required for both text and image documents are very close. For example, using all 306 features for classification requires around 30 min. However, using selected 222 features for classification needs around 20 min. According to Section 3.1’s description, the time expense is based on ten times of training and testing in order to get the average results for classification. Therefore, in average, one cycle of training and testing only need 2 min by selected 222 features.

The experimental system is using Intel i5-2400CPU @3.10 GHz, Window 7 64-bit system with 8G RAM. The whole computation software and hardware system could be further optimized to speed up the entire processes.

On the other hand, CNN based computation generally requires higher level of computation specification and graphics processing unit (GPU) is especially important. The experimental system is using Intel i7-7700CPU @3.60 GHz, Window 10 64-bit system with 16G RAM. GPU is GeForce GTX 1070 with 8G RAM. Table 12 tabulates the simulation results for Japanese character “あ” by different layer’s CNNs system. The training time is about 40 min for 7 layer system and 76 min for 13 layer system. As expected, the testing time is much shorter for CNNs based system than feature based SVM system. For example, the testing time is only 17.727 s for 7 layer system and 22.428 s for 13 layer system.

Due to the limit of the current research resources, both methods are implemented in different stage and computation systems since SVM is long established and deep learning technique is new and under investigation. As mentioned above, the results in Fig. 14 and Table 12 just demonstrate the computation requirement for the classification applications. The whole system could be further improved for better hardware and software optimization. In addition, the cloud computing

Table 13
Comparison of average classification accuracy.

Classification technique	Text		Natural image	
	Scanned image	Microscopic image	Scanned image	Microscopic image
SVM	98.72%	99.96%	99.95%	99.98%
CNNs (7 layer)	98.41%	97.37%	99.93%	97.7%
		(13 layer)	(7 layer)	(13 layer)

could be implemented to share the computation load. It may also facilitate the application for real-time identification using edge computing.

• Accuracy analysis

Besides the discussion of the calculation time, the accuracy of the classification capability for the identification system is more critical and concerted in real applications. As suggested in [28], LBP feature based SVM system performs well for the microscopic images and this study adopts those features for simulation. The results are tabulated in Table 13. By averaging the results from Tables 4, 5 and 6, 7 respectively, Table 13 tabulates the comparison of the forensic classification results for scanned images and microscopic images by two different systems, i.e. feature based SVM system and deep learning system.

Feature based SVM system can achieve accuracy at 98.72% and CNNs can achieve accuracy at 98.41% by 7 layer system for text scanned image. Both results are very comparable. For Lena, Peppers and Baboon images, SVM based system can achieve average accuracy at 99.95% and CNNs can achieve average accuracy at 99.93% by 7 layer system. Both results are also comparable at high rates.

However, for microscopic images of text document, SVM based system can achieve accuracy at 99.96% and CNNs can only achieve accuracy at 97.37% by 13 layer system in this study. There is about 2% difference in accuracy. For microscopic input images of Lena, Peppers and Baboon, SVM based system can achieve average accuracy at 99.98%, but CNNs can only achieve average accuracy at 97.70% by 13 layer system. Even the accuracy rates are high, there is still 2% difference between both systems. Apparently, the results from feature based SVM system are superior to the results using deep learning system under current study for microscopic image input.

From the experimental results, the data suggest that both system can behave comparable classification performance for scanned documents. However, there exists a performance gap between two systems for documents based on microscopic images. Therefore, the classification capability of deep learning system need to be improved in order to match the performance by feature based SVM system for microscopic input images. Accordingly, several issues could be considered as following:

1. Due to the fair comparison, there are only 500 samples for training and 300 samples for testing in Experiment 4.2 for both systems. This setting is the same as previous studies in [9–12,19,20,28]. Current setting of deep learning system behaves as well as the feature based SVM system for the scanned images. Further improvement is needed for the microscopic images as the input. Under such constraints, this study has tried different parameters to get the best design of the deep learning system as shown in Table 3. Based on the nature of the requirement for deep neural networks, the success generally bases on the learning capability with large amount of data. This study essentially can enlarge the sample number of training for deep learning system. However, such a change could be unfair to compare the results with previous studies and this could be a conflicted choice for implementation.
2. The image patch used in [28] study is non-overlapping at size 45×45 and already provides enough textural information for feature based SVM system. If only non-overlapping patches applied for deep learning system, the results shown in Table 9 are

not comparable to the results shown in Table 11. Even the input image is the overlapping patch at 90×90 , the results of Table 10 are improved by the augmented information, but still not as good as shown in Table 11. The reason might be two reasons: the first one is that the deep learning system need to be improved. The second one is not enough data for training. Therefore, the area of overlapping could be enlarged.

3. In other research area, deep learning based classification technique has been applied in breast cancer histopathological images [40]. Spanhol et al. [40] adopted CNNs architecture to classify breast tissue biopsy samples in benign and malignant tumors, using multiple magnifications to get approximately 2000 images. In their work, 32×32 and 64×64 pixels patches were extracted from the initial images and used for training the CNNs. As [41] suggested, the dataset is divided into training (70%) and testing (30%) which takes higher percentage of samples than this study. For the $200\times$ magnification, the achieved accuracy was approximately 84%. The authors reported an accuracy decrease for higher magnifications, and implied that their CNN architecture cannot extract relevant features for higher magnifications. Under current study, feature based SVM classification can adjust the features selected for images under different magnifications. Even the input images are different in this study, the experimental outcomes are quite similar to the relevant deep learning based researches. Therefore, there is still room of improvement for the deep learning based classification system, while microscopic images are applied.
4. Since the breakthrough in 2012 ImageNet competition [42], Deep Neural Network (DNN) emerges as a prominent technique for object detection and image classification at large scale. Several other DNNs with increasing complexity have been submitted to the challenge in order to achieve better performance. For example, AlexNet [8] had a very similar architecture as LeNet by LeCun Y. et al. [32] but was deeper, with more filters per layer, and with stacked convolutional layers. The GoogLeNet [43] used a CNN inspired by LeNet but implemented a novel element which is dubbed an inception module. This module is based on several very small convolutions in order to drastically reduce the number of parameters. VGGNet [44] consists of 16 convolutional layers and is very appealing because of its very uniform architecture. Residual Neural Network (ResNet) by He K. et al. [45] introduced a novel architecture with “skip connections” and features heavy batch normalization.

In general, those highly acclaimed deep learning algorithms are basically designed for computer vision and image recognition with large scale labeled data samples. However, the data size of printed sources are basically small scale since the digital data need to be printed, scanned, extracted and tagged for reference, and huge human involvement is required. Besides, extra time and works are needed to seek the best parameter settings for the deep learning structures. Since many advanced and complicated deep learning structures are generally based on CNN, the authors had implemented the model, build the structure step by step, and fine tune the parameters to get the highest accuracy for printer source identification in this study. Therefore, advanced investigation improved the experimental data of [46] since deep learning generally requires significant learning procedures to get the best results. Hence CNN model is feasible for forensic study, future researchers could applied above mentioned DNN model like GoogLeNet, VGGNet, ResNet or new structures to validate their feasibility, and improve their performance for digital forensics of printer source identification.

In conclusion, the experimental results from this study demonstrate that the classification outcomes of deep learning based technique can match the conventional handcrafted feature based classification approach, while the input is scanned images. The advantage of deep learning can

reduce the human intervention and the system can extract and organize the discriminative information from the data automatically. On the other hand, there still exists a gap between deep learning based method and the feature based SVM classification regarding the classification accuracy, while the input is the microscopic images. Since the deep learning relies on large data for good training, it is suggested that the number of training samples for microscopic images need to be increased which could eventually match the performance of the feature based SVM classification.

5. Conclusion

This research engages in the forensic study for printed document source identification. This study has investigated the scanned and microscopic images in printed source identification, by feature based SVM classification system and deep learning system. Prior researches have implemented scanners as the digitizing technique to resolve very fine printed document. On the other hand, the performance of microscopic techniques can retrieve the shape and surface texture of a printed document with detailed micro structures among printer sources. From the experimental results, both classification systems can achieve the state-of-the-art performance and they are both comparable for scanned documents either texts or natural images. However, the results from feature based SVM system are superior to the results using deep learning system under current study based on microscopic image input. Several issues have been discussed in order to improve the deep learning system, for example, whether the structure of CNNs should be modified, the limited field of view after magnification by microscope and limited data for training. While data and time is constrained, it is still valuable to use existing known features for initial classification and retrieve the decision with high accuracy.

Regarding the future research, it is still a continuous work to explore more useful features to expand the feature space. Deep learning based system could be further explored and optimized. Both systems should be constantly evaluated and compared for the best interest in universal applications. New research direction for cancer classification of medical image is creating new avenues for the development in early cancer detection. Importantly, micro imaging studies conducted on cancer classification have strongly suggested that, in addition to benefits in cancer identification, it also has advantages to determine the appropriate treatment to avoid the risk of errors for the patients. The techniques developed in this study could be leveraged into medical fields.

Acknowledgment

This work was partially supported by the Ministry of Science and Technology in Taiwan, under MOST104-2410-H-009-020-MY2, MOST106-2410-H-009-022 and MOST107-2410-H-009-019-MY2.

References

- [1] J.A. Lewis, *Forensic Document Examination: Fundamentals and Current Trends*, Elsevier, Oxford, 2014, <http://dx.doi.org/10.1016/B978-0-12-416693-6.12001-6>.
- [2] N. Khanna, E.J. Delp, Intrinsic signatures for scanned documents forensics: effect of font shape and size, in: *Proceedings of 2010 IEEE International Symposium on Circuits and systems, ISCAS*, 30 May– 2 June, 2010. <http://dx.doi.org/10.1109/ISCAS.2010.5537996>.
- [3] G.N. Ali, A.K. Mikkilineni, P.J. Chiang, G.T. Allebach, E.J. Delp, Intrinsic and extrinsic signatures for information hiding and secure printing with electrophotographic devices, in: *International Conference on Digital Printing Technologies*. New Orleans, LA, USA; 28 Sept–3 Oct, 2003, pp. 511–515.
- [4] R.C. Gonzales, R.E. Woods, *Digital Image Processing*, third ed., Prentice Hall, New Jersey, 2008.
- [5] R.C. Gonzales, R.E. Woods, S.L. Eddins, *Digital Image Processing Using MATLAB*, second ed., Gatesmark, United States, 2009.
- [6] C.W. Hsu, C.C. Chang, C.J. Lin, *A Practical Guide to Support Vector Classification*, National Taiwan University, Taipei, 2003, <http://www.csie.ntu.edu.tw/~cjlin/papers/guide/guide.pdf>.

- [7] Bishop. C.M., *Pattern Recognition and Machine Learning*, Springer, New York, 2006.
- [8] A. Krizhevsky, I. Sutskever, G. Hinton, ImageNet classification with deep convolutional neural networks, *Processing of International Conference on Neural Information Processing Systems, NIPS*, Vol. 1, 2012, pp. 1097–1105.
- [9] A.K. Mikkilineni, O. Arslan, P.J. Chiang, R.M. Kumontoy, J.P. Allebach, G.T. Chiu, Printer forensics using SVM techniques, in: *Intl. Conference on Digital Printing Technologies*, 2005, pp. 223–226.
- [10] M.J. Tsai, J.S. Yin, I. Yuadi, J. Liu, Digital forensics of printed source identification for Chinese characters, *Multimedia Tools Appl.* 73 (2014) 2129–2155, <http://dx.doi.org/10.1007/s11042-013-1642-2>.
- [11] M.J. Tsai, J. Liu, 2013 Digital forensics for printed source identification, in: *IEEE International Symposium on Circuits and Systems, ISCAS*, May, pp. 2347–2350, <http://dx.doi.org/10.1109/ISCAS.2013.6572349>.
- [12] A. Ferreira, L.C. Navarro, G. Pinheiro, J.A.D. Santos, A. Rocha, Laser printer attribution: Exploring new features and beyond, *Forensic Sci. Int.* 247 (2015) 105–125, <http://dx.doi.org/10.1016/j.forsciint.2014.11.030>.
- [13] A. Ferreira, L. Bondi, L. Baroffio, P. Bestagini, J. Huang, J.D. Santos, S. Tubaro, A. Rocha, Data-driven feature characterization techniques for laser printer attribution, *IEEE Trans. Inf. Forensics Secur.* 12 (8) (2017).
- [14] E. Kee, H. Farid, Printer profiling for forensics and ballistics, in: *ACM Workshop on Multimedia and Security*, 2008, pp. 3–10.
- [15] Y. Wu, X. Kong, X. You, Y. Guo, Printer forensics based on page document's geometric distortion, in: *Intl. Conference on Image Processing, ICIP*, Cairo, 2009, pp. 2909–2912, <http://dx.doi.org/10.1109/ICIP.2009.5413420>.
- [16] J.H. Choi, H.Y. Lee, H.K. Lee, Color laser printer forensic based on noisy feature and support vector machine classifier, *Multimedia Tools Appl.* 67 (2013) 363–382, <http://dx.doi.org/10.1007/s11042-011-0835-9>.
- [17] D.G. Kim, H.K. Lee, Color laser printer identification using photographed halftone images, in: *Proc. of EUSIPCO, IEEE*, Lisbon, 2014, pp. 795–799.
- [18] S.J. Ryu, K.Y. Lee, D.H. Im, J.H. Choi, H.K. Lee, Electrophotographic printer identification by halftone texture analysis, in: *IEEE Intl. Conference on Acoustics Speech and Signal Processing, ICASSP*, 2010, pp. 1846–1849, <http://dx.doi.org/10.1109/ICASSP.2010.5495377>.
- [19] A.K. Mikkilineni, P.J. Chiang, G.N. Ali, G.T. Chiu, J.P. Allebach, E.J. Delp, Printer identification based on textural features, in: *Intl. Conference on Digital Printing Technologies*, 2004, pp. 306–311.
- [20] A.K. Mikkilineni, J.P. Chiang, G.N. Ali, G.T. Chiu, J.P. Allebach, E.J. Delp, Printer identification based on graylevel co-occurrence features for security and forensic applications, in: *Intl. Conference on Security, Steganography and Watermarking of Multimedia Contents*, 2005, VII, *Proc. SPIE*. Vol. 5681, pp. 430–440, <http://dx.doi.org/10.1117/12.593796>.
- [21] O. Bulan, J. Mao, G. Sharma, Geometric distortion signatures for printer identification, in: *International Conference on Acoustics, Speech and Signal Processing, ICASSP*, 2009, Taipei, pp. 1401–1404, <http://dx.doi.org/10.1109/ICASSP.2009.4959855>.
- [22] S. Tong, D. Koller, Support vector machine active learning with applications to text classification, *J. Mach. Learn. Res.* (2001) 45–66.
- [23] K.I. Kim, K. Jung, S.H. Park, H.J. Kim, Support vector machines for texture classification, *IEEE Trans. Pattern Anal. Mach. Intell.* 24 (11) (2002) 1542–1550, <http://dx.doi.org/10.1109/TPAMI.2002.1046177>.
- [24] D. Yu, L. Deng, *Automatic Speech Recognition: A Deep Learning Approach*, Springer-Verlag, London, 2015.
- [25] Y. Freund, R.E. Schapire, A decision-theoretic generalization of on-line learning and an application to boosting, *J. Comput. System Sci.* 55 (1) (1997) 119–139.
- [26] I. Buciu, Demonstrating the stability of support vector machines for classification, *Signal Process.* (86) (2006) 2364–2380.
- [27] W. Jeevani, Performance degradation in boosting, in: *International conf. MCS 2001: multiple classifier systems*, pp. 11–21.
- [28] Tsai. M., I. Yuadi, Digital forensics of microscopic images for printed source identification, *Multimedia Tools Appl.* 77 (7) (2018) 8729–8758.
- [29] D. Hubel, T. Wiesel, Receptive fields, binocular interaction and functional architecture in the cat's visual cortex, *J. Physiol.* 160 (1) (1962) 106–154.
- [30] G. Hinton, R. Salakhutdinov, Reducing the dimensionality of data with neural networks, *Science* 313 (5786) (2006) 504–507.
- [31] J. Markoff, How Many Computers to Identify a Cat? 16, 000, *The New York*. Retrieved June 22, 2012, from <https://mobile.nytimes.com/2012/06/26/technology/in-a-big-network-of-computers-evidence-of-machine-learning.html>.
- [32] Y. Lecun, L. Bottou, Y. Bengio, P. Haffner, Gradient-based learning applied to document recognition, *Proc. IEEE* 86 (11) (1998) 2278–2324.
- [33] M. Lin, Q. Chen, S. Yan, *Network in Network*, Cornell University Library, 2014, p. 10, <arXiv:1312.4400> [cs.NE].
- [34] E. Rumelhart, E. Geoffrey, J. Ronald, Learning representations by back-propagating errors, *Nature* 323 (1986) 533–536.
- [35] R.M. Haralick, K. Shanmugam, I. Dinstein, Textural features for image classification, *IEEE Trans. Syst. Man Cybern., SMC* 3 (6) (1973) 610–621.
- [36] G. Costa A.F. Humpire-Mamani, A.J.M. Traina, An efficient algorithm for fractal analysis of textures, in: *SIBGRAPI Conference on Graphics, Patterns and Images*, August, 2012, Ouro Preto, pp. 39–46, <http://dx.doi.org/10.1109/SIBGRAPI.2012.15>.
- [37] T. Mäenpää, M. Pietikäinen, *Texture analysis with local binary patterns*, third ed., World Scientific, Singapore, 2004, pp. 115–118.
- [38] Z. Qiu, J. Jin, H.K. Lam, Y. Zhang, X. Wang, A. Cichocki, Improved SFFS method for channel selection in motor imagery based BCI, *Neuro Comput.* 207 (2016) 519–527, <http://dx.doi.org/10.1016/j.neucom.2016.05.035>.
- [39] P. Pudil, J. Novovicova, J. Kittler, Floating search methods in feature selection, *Pattern Recognit. Lett.* 15 (1994) 1119–1125.
- [40] F.A. Spanhol, L.S. Oliveira, C. Petitjean, L. Heutte, Breast cancer histopathological image classification using convolutional neural networks, in: *International Joint Conference on Neural Networks*, 2016, Vancouver, pp. 2560–2567.
- [41] F.A. Spanhol, L.S. Oliveira, C. Petitjean, L. Heutte, A dataset for breast cancer histopathological image classification, *IEEE Trans. Biomed. Eng.* 63 (7) (2016) 1455–1462.
- [42] O. Russakovsky, et al., *Imagenet large scale visual recognition challenge*, *Int. J. Comput. Vis.* 115 (3) (2015) 211–252.
- [43] C. Szegedy, Going deeper with convolutions, in: *IEEE Conference on Computer Vision and Pattern Recognition (CVPR)*, 2015, <http://dx.doi.org/10.1109/CVPR.2015.7298594>.
- [44] K. Simonyan, A. Zisserman, Very deep convolutional networks for large-scale image recognition, in: *IEEE Conference on Computer Vision and Pattern Recognition (CVPR)*, 2015, [arXiv preprint arXiv:1409.1556](arXiv:1409.1556).
- [45] He K., et al., Deep residual learning for image recognition, in: *IEEE Conference on Computer Vision and Pattern Recognition, CVPR*, 2016, pp. 770–778.
- [46] M.J. Tsai, I. Yuadi, Y.H. Tao, Decision-theoretic model to identify printed sources, *Multimedia Tools Appl.* 77 (20) (2018) 27543–27587.